Supporting Information

Ofek et al. 10.1073/pnas.1004728107

SI Text

Materials and Methods. ***Semiautomated Design of Epitope Scaffolds.*** The overall design procedure consisted broadly of "matching" and "design" stages. The computational work flow was carried out by custom shell scripts (1). In the "matching" stage, the Protein Data Bank (PDB) (2) was searched for scaffolds with backbone-structural similarity to any segment of the 2F5-bound gp41 peptide spanning the range 659–669, and the initial structural matches were filtered based on antibody clash. PISCES (3) was used to cull the PDB of November 11, 2004, down to 14,383 chains of more than 50 residues with resolution better than 3.0 Å. MAMMOTH (4) was used to search the culled PDB for sequence-independent structural matches based on Cα coordinates. Structural matches were ranked by the ratio of rmsd to the number of superimposed residues (rmsd/nsup). RosettaDesign (5, 6) was then used for clash-checking. The best 5% of matches by rmsd/nsup (700 matches with rmsd/nsup < 0.132) were evaluated for steric clash (Rosetta score "E_{rep}") between the scaffold backbone (side-chains mutated to glycine) and the antibody (all atoms retained), with the relative orientation of scaffold and antibody determined by the structural superposition of the epitope segment onto the scaffold. The 25 scaffolds with the least clash were retained for further analysis; these scaffolds had E_{rep}(bind) less than 200 score units above the E_{rep}(bind) measured for the 2F5-gp41 crystal structure with gp41 mutated to glycine, where $E_{rep}(\text{bind}) = E_{rep}(\text{complex}) - E_{rep}(\text{partner1}) - E_{rep}(\text{partner2})$. Scaffolds with higher clash values were judged to require too many severe atomic overlaps with antibody to allow binding. Five scaffolds with cofactors were then eliminated. Many of the remaining 20 scaffolds were oligomeric in their native state, so the clash analysis was repeated with the native oligomers, resulting in the final selection of five scaffolds—1LGYa (ES1), 1KU2a (ES2), 2MATa (ES3), 1IWLa (ES4), 1D3Bb (ES5). In two of the five chosen scaffolds, the epitope was occluded on the native oligomer [ES2 homodimer (7) and ES5 hetero-dimer (8)], but in both cases we judged that oligomerization was not essential to maintain the scaffold structure and that the mutations associated with epitope transplantation could result in monomeric proteins with an exposed 2F5 epitope.

In the "design" stage, epitope side chains were transplanted to the appropriate positions on the remaining scaffolds, and further mutations were designed on each scaffold to minimize nonepitope interactions with antibody and to optimize stability. RosettaDesign was used to pack side chains on the scaffold backbone, with side-chain conformations restricted to those contained in the backbone-dependent rotamer library of Dunbrack and Cohen (9) or to native scaffold rotamer conformations, and an energy function dominated by a 12-6 Lennard–Jones potential, a geometry-dependent hydrogen bond potential, and an implicit solvation model as detailed in the supplementary information for Kuhlman et al. 2003 (6). Antibody-contacting epitope residues (E659, L661, E662, D664, K665, W666, A667, L669) were transplanted to corresponding scaffold positions according to the MAMMOTH structural alignment where possible, while scaffold positions adjacent to the epitope or to the antibody were designed to accommodate epitope side chains and avoid interactions with antibody, and all other scaffold positions were assigned native-scaffold amino-acid rotamers. On average, eight epitope residues were transplanted and eight additional mutations were made to each of these scaffolds.

Subsequent to the original design of the epitope scaffolds, the protocol was improved to include transplantation of native epitope rotamers to each scaffold, followed by energy minimization (10) of rigid-body and rotameric torsional degrees of freedom at the scaffold-antibody interface, prior to design of scaffold positions outside the epitope. Scaffold models analyzed in this manuscript were produced by the updated protocol using the originally designed scaffold sequences.

Cloning, Expression, and Purification of Epitope Scaffolds.

Cloning.
Plasmids for the expression of all scaffolds were derived by de novo gene synthesis, followed by subcloning into the CMV/R expression plasmid (11) (GenScript, Bionexus). All constructs were appended with an N-terminal CD5 leader sequence for secretion from mammalian cells, as well as with a C-terminal Hisx6 and C9 (TETSQVAPA) tags, the latter of which reacts with the 1D4 mouse antibody (12). Given that several 2F5-epitope scaffolds (ES1, ES3, and ES5) did not express or secrete in the mammalian expression system, the genes were subcloned into the bacterial expression plasmid pET-17b (Novagen). PCR reactions were carried out with primers that introduced two unique restriction sites (Nde I and BamH I) to facilitate the ligation of the PCR products into the pET-17b expression vector. Ligation of the PCR products and vector pET-17b was carried out after digestion. The plasmids were transformed into Rosetta BL21 E. coli cells. Addition of a universal heterologous T-cell helper epitope (AFKVAAWTLKAAA) to the scaffolds was undertaken either by QuickChange site-directed mutagenesis (Stratagene) for ES3, or by de novo gene synthesis for ES2 and ES5. A plasmid for a shorter fragment of ES2 was cloned using QuickChange site-directed mutagenesis (Stratagene) to add a stop codon after residue 271.

Expression.
Transient transfection of epitope-scaffold mammalian expression plasmids into adherent HEK 293 cells or Freestyle 293F cells (Invitrogen) was undertaken using Lipofectamine or 293fectin transfection reagents, respectively (Invitrogen). For 293F Freestyle expression, cells were grown in 2L flasks to a density of 1.2×10^6 cells per ml and transfected with 250-500 μgs of plasmid DNA per liter of 293 Freestyle growth medium (Invitrogen). Cell culture supernatants were collected 4–5 days after transfection, centrifuged at $3{,}500 \times g$ to remove cell debris and filtered using a 0.22 micron filter unit. Of the five scaffolds, ES2 and ES4 were successfully secreted from mammalian cells.

For the remaining scaffolds, ES1, ES3, and ES5, bacterial expression was undertaken. A 50 ml culture of Rosetta BL21 *E.coli* transformed with the expression vector was grown overnight at 37 °C. The next morning a 1L culture was grown from the 20 ml overnight culture to an OD_{600} of 0.6–1.0 and induced with IPTG to a final concentration of 1 mM. After growth for 6 h, the cells were harvested and pelleted by centrifugation at $5{,}000 \times g$.

Purification.
Mammalian expressed scaffolds (ES2 and ES4) were purified from the supernatants through a combination of a chelating (nickel), affinity (2F5-antibody), and size-exclusion chromatography (Superdex 75 or 200). In brief, 1L supernatants were either applied directly to a nickel column or first buffer-exchanged into PBS, pH 7.4. Binding was undertaken in 500 mM NaCl, 20 mM Tris-Cl, pH 8.0, 20 mM imidazole, followed by washes and elution with binding buffer supplemented with 40 and 500 mM imidazole, respectively. Eluates were concentrated, buffer-exchanged into PBS (Amicon Ultra centrifugal filter devices, Millipore), and

then loaded onto a 2F5 antibody affinity column. Samples were eluted using Pierce IgG elution Buffer, pH 2.8, followed by rapid pH adjustment with Tris-Cl, pH 8.5-9. Eluates were pooled, concentrated, and then loaded onto a size-exclusion column (Superdex 75 or 200).

All bacterially expressed scaffolds—ES1, ES3, and ES5—segregated into inclusion bodies, and purification was undertaken first by lysing the bacterial cell pellet with Bugbuster reagent containing lysozyme and nucleases (Novagen), followed by centrifugation at 10,000 × *g* to pellet the inclusion bodies. Inclusion bodies were resuspended overnight under denaturing conditions of 8 M urea, 20 mM Tris-Cl, pH 8.0, 1 mM beta-mercaptoethanol or DTT, and then centrifuged and filtered, and loaded onto a nickel column equilibrated with binding buffer comprised of 8 M urea, 500 mM NaCl, Tris-Cl, pH 8.0, imidazole 10 mM. Loaded samples were then washed with binding buffer supplemented with 40 mM imidazole, and eluted with binding buffer supplemented with 300–500 mM imidazole. Eluates were concentrated to 1 ml using an Amicon Ultra concentrator (Millipore). Refolding of concentrated eluates was performed overnight at 4 °C by quick dilution (1:100) into refolding buffer comprised of 50 mM Tris-Cl, pH 8.0, 250 mM NaCl, 500 mM L-Arginine, 0.1 mM glutathione reduced, 0.01 mM glutathione oxidized, 0.03% N-laurylsarcosine and 0.1 mM $ZnCl_2$. Refolded samples were then concentrated to 5–7 ml using Centricon plus-80 (Millipore) and dialyzed into PBS supplemented with 125 mM NaCl. For ES3 and ES5, a further round of purification was undertaken by applying the samples to a 2F5 antibody affinity column. The ES1 scaffold did not remain soluble after elution from the affinity column, and was therefore only subjected to nickel column purification.

Surface–Plasmon Resonance. For the binding of 2F5 to the epitope scaffolds, the scaffolds were directly immobilized onto Biacore CM5 sensor chips (GE Healthcare) to final surface densities of ~500 RU. 2F5 antigen-binding fragment (Fab) was then used as analyte at concentrations ranging from 0.5 nM to 500 nM, at 2-fold serial dilutions, with association and dissociation phases of up to 5 min, at a flow rate of 30 ml/ min. To determine binding affinities of antibodies 2F5, 11f10 and 6a7 to gp41 peptides, the antibody IgGs were immobilized directly to CM5 sensor chips at surface densities of ~4,000–5,000 RU, and the gp41 MPER-C9 peptide (EQELLELDKWASLGGTETSQVAPA) or the MPER-C9-cyclized peptide (EQELLE-Dap-DKWDSLGGTETSQ-VAPA) were flowed over as analyte at 2-fold increasing concentrations ranging from 0.5 nM to 500 nM. To determine binding constants, the sensograms plotted in Figs. S2 and S4 were fit with 1:1 Langmuir models using Biacore BiaEvaluation Software (GE Healthcare) or Scrubber 2 (Biologic). In all cases, Biacore HBS-EP buffer was used (10 mM Hepes, pH 7.4, 150 mM NaCl, 3 mM EDTA, 0.01% P-20), and replicates of the lowest dilution were performed.

Isothermal Titration Calorimetry. Calorimetric measurements were performed using Microcal VP-ITC or ITC-200 at 37 °C. All pairwise 2F5/ligand samples were dialyzed extensively into identical batches of 1X or 0.5X of the solution 350 mM NaCl, 2.5 mM Tris-Cl, pH 7.1 or PBS supplemented with 125 mM NaCl. 2F5 IgG was placed into the calorimeter cell at a concentration of 1–2 μM, and the scaffolds or peptides were injected as titrants. Between 25–30 injections were performed per run, at 5–10 μl per injection. Heats of dilution of the titrants were assessed based on control experiments of titrant into buffer and buffer into macromolecule, or by analysis of the heats observed for the last set of injections after saturation. Concentrations of all ligands were determined using A_{280} absorbance and known extinction coefficients for each of the proteins. If measured concentrations yielded fits of the ITC data that were inconsistent with expected stoichiometries of $n = 2$ for an IgG interaction, effective active concentrations of the epitope scaffolds were assessed based on achieving stoichiometries of $n = 2$. These effective concentrations were then used in obtaining the final thermodynamic parameters. With the exception of the ES5 scaffold, the effective concentrations of all titrants were within ~90% of the concentrations measured using A_{280} absorbance. For ES5, based on expected stoichiometry, the effective concentration was predicted to be 25–30% that measured by absorbance. Due to the large discrepancy in the measured and effective concentrations for ES5, the experiment for this scaffold was also performed in the reverse format, with 2F5 Fab as titrant and ES5 present in the cell. In this case, the effective concentration of ES5, as predicted by stoichiometry of binding, came to 38% that measured by A_{280}, confirming to within 10% the effective concentration predicted in the first format (ES5 as titrant). The estimated effective concentrations of the scaffolds were therefore as follows: ES2, 40 μM; ES4, 24 μM; ES5, 135 μM; MPER WT peptide, 25 μM; MPER cyclized peptide, 30 μM. Profiles were fit using Origin Ver. 7.0 (Microcal).

Generation of Animal Sera. Sera generated from immunogens which had the gp41 MPER inserted into flexible contexts were generated by injecting rabbits with free or cyclized MPER peptides linked to KLH through thiol linkage (NEQELLELDKW-ASLW GGC or EQELLE-Dap-DKWDSLW GGC, respectively) (Washington Biotechnology). Guinea pig sera generated previously by insertion of the gp41 MPER sequence LLELDKWA into a flexible surface loop on HIV-1 gp140 were also used, and were a kind gift from B. Chakrabarti and G. Nabel (13).

Sera elicited by epitope scaffolds were generated by intramuscular injection of Hartley guinea pigs (females, ~10 weeks of age) with 20 μg of affinity purified protein formulated in either a GlaxoSmithKline Adjuvant System AS01B or a combination of Alum (2% Aluminum Hydroxide gel, 50 μl per animal) with CpG (250 μg per animal) at 4 week intervals. The protein-adjuvant emulsion was always prepared within 1 h of inoculation into animals. The first four inoculations were all homologous protein. Subsequent inoculations were either homologous or heterologous protein. Bleeds were collected 7–10 days after each inoculation. Serum was collected and incubated at 55 °C for 1h to heat-inactivate complement and stored at −80 °C until subjected to analysis.

Analysis of Animal Sera.

ELISA profiles.
100 ng/well of mouse monoclonal antibody 1D4 (12) (with specificity to C9 tags) was adsorbed overnight at 4 °C onto a Maxisorp plate (Nunc) in PBS. The next day plates were washed five times with wash buffer composed of PBS supplemented with 0.2% Tween 20, and then blocked for 2 h at 25 °C in PBS supplemented with 5% dry-milk powder (Difco) and 5% heat-inactivated Fetal Bovine Serum (Sigma or Gibco). Following a wash step, scaffolds or peptides in PBS, all of which had a covalently linked C9 tag at the C terminus, were loaded onto the plates at 10X molar excess with respect to the adsorbed 1D4 antibody and incubated for 1h at 25 °C. Following a wash step, serum was added at fivefold serial dilutions (1:50 to 1:781250) in PBS, 0.2% Tween 20 and incubated for 1 h at 25 °C. Pooled preimmune sera per animal group were also tested (at the same serum dilutions), as was antibody 2F5, at fivefold serial dilutions from 5 μg/ml to 6.4×10^{-05} μg/ml. Plates were washed five times with wash buffer followed by incubation with a donkey secondary anti-guinea pig immunoglobulin (H + L) (Jackson Labs) at a 1:10000 dilution in PBS, 0.2% Tween 20 for 1 h at 25 °C. Plates were washed again, followed by addition of 100 uL of the colorometric TMB (3,3′,5,5′-tetramethylbenzidine) peroxidase enzyme immunoassay substrate (Bio-Rad) to each well. The reactions were

stopped with 100 μL of 0.1N H_2SO_4per well. Optical density was read on a microplate reader at 450 nm using Softmax software (Molecular Devices). All samples were performed in duplicate. GraphPad Prism Version 5.0 was used to fit four parameter logistic curves to all ELISA profiles.

Analysis of ELISA profiles of flexible MPER sera.
Means of replicate EC_{50}s and standard deviations of the means are reported. In cases where the ELISA curves were too flat to fit, resulting in lack of convergence or ambiguity, constraints were added to limit the tops of the fits so that an EC_{50} could be interpolated. This was the case for curves of recognition of ES2 by Flexible MPER B (2 replicates); for recognition of ES4 by Flexible MPER B (1 replicate); for recognition of ES1 by Flexible MPER B (2 replicates); and for recognition of the negative control 1D4 antibody by Flexible MPER A (1 replicate) and Flexible MPER B (2 replicates). In the case of recognition of ES2 by Flexible MPER A, the curve was too flat to fit even in the presence of constraints, and the EC_{50} was set to the highest dilution of 7.6.

Analysis of ELISA profiles of epitope scaffold elicited sera.
Mean EC_{50}s of the individual sera were obtained by applying the fits to all replicates per scaffold per bleed. EC_{50}s calculated per scaffold (Fig. 2*C*) entailed 2 replicates each for scaffolds ES1, ES3, ES4, and 8 replicates each for scaffolds ES2 and ES5. A constraint on the top of the fits to be less than 5 was applied in all cases. In cases where the curves of individual replicates were too flat to obtain a proper fit of the data, the replicates were excluded from the analysis. This was the case for profiles ES3.AS01B.Post 2 (1 replicate), ES1.AS01B2.Post 2 (1 replicate), ES2.Alum/CpG.Post 4 (1 replicate), ES2.AS01B.Post 2 (1 replicate), ES2.AS01B.Post 4 (1 replicate), ES2.TH.Alum/CpG.Post 4 (1 replicate), ES2.TH. AS01B.Post 2 (1 replicate), ES2.TH.AS01B.Post 4 (2 replicates), and ES4.Alum/CpG.Post 2 (1 replicate).

Analysis of alanine scan ELISA profiles.
EC_{50}s of alanine-interrogated ELISA profiles were determined as described above (per replicate). In cases where the responses were too flat to accurately obtain a fit, replicates were excluded from the analysis. All EC_{50}s were normalized relative to the EC_{50} of wild-type MPER peptide, as defined by the peptide for which position 667 of gp41 is an alanine. To determine similarity of profiles to 2F5, an *R*-value calculation was used, as defined by the expression $R = (\sum_{i=658}^{670} |EC50_i^{\text{ES Sera}} - \overline{EC50_i^{2F5}}|)/(\sum_{i=658}^{670} |EC50_i^{\text{ES Sera}}|)$, where *i* is the residue at which the peptide is mutated to alanine. Unique *R*-values were computed from the normalized EC_{50} data for each technical replicate of each serum, then mean *R*-values and standard errors were computed from the two technical replicate *R*-values. Resampling tests were computed in R 2.10 (http://www.R-project.org) to determine if any of the test sera were significantly similar to the 2F5-MAb profile. Bootstrap samples of the normalized EC_{50} measurements were collected from the pool of 41 test sera (all sera except for MAb 2F5) at each of the 13 residues, then mean *R*-values were computed from the resampled normalized EC_{50} data to simulate a distribution of all possible *R*-values. Mean *R*-values estimates from the individual sera and from select groups of sera were compared to the histogram and *p*-values were computed as the proportion of the area under the histogram to the left of the mean *R*-factors. A Bonferroni adjustment was used to account for multiple comparisons (30); *p*-values were only considered statistically significant if $p < 0.05/58 = 0.0008621$, yielding two profiles that were statistically significant in their similarity to 2F5: ES2.TH.AS01B.Post 6 and ES2.TH.Alum.CpG.Post 6. A less conservative False Discovery Rate (FDR) step-up adjustment was also applied (31), yielding six profiles that were statistically significant in their similarity to 2F5 with a 3.75% false discovery rate: ES2.TH.AS01B.Post 6, ES2.TH.Alum.CpG.Post 6, ES5.Alum.CpG.Post 2, ES1.AS01B2.Post 6, ES5.TH.AS01B.Post 4, ES5.Alum.CpG.Post 6.

Because the distribution of the resampled *R*-factors was approximately normally distributed, Student's t-tests were used to compare the mean *R*-values from several groups of sera. A Bonferroni adjustment was used to account for multiple comparisons (30); *p*-values were only considered statistically significant if $p < 0.05/18 = 0.0027778$. Only the comparison of *R*-values of groups that did or did not possess a T-helper epitope, was statistically significant, with $p = 0.0154$ after Bonferroni multiplication by 18. The results of the Student's t-test were confirmed by Mann-Whitney and Kruskal–Wallis tests.

Generation of Graft-Specific Monoclonal Antibodies Ulsing Epitope Scaffolds. Balb/c mice were inoculated subcutaneously with 20 μg of affinity purified protein (ES5, ES1) formulated in a combination of Alum (2% Aluminum Hydroxide gel, 50 μL per animal) with CpG (250 μg per animal) at 2 week intervals (ProSci). Serum was collected 7–10 days after each inoculation. The protein-adjuvant emulsion was always prepared within 1 h of inoculation into animals. ELISA IgG titers measured using selection antigens ES2 (no tags) and MPER peptide (EQELLELDKWASLWNWFDITKWLWYIKKKKGSKKK) were used to determine mice that were to be sacrificed to proceed with fusion of spleen. Secondary selections of positive clones were carried out using selection antigens ES2, ES3, and ES4.

The 11f10 and 6a7 antibodies were sequenced by a combination of N-terminal Edman sequencing followed by reverse transcriptase polymerase chain reaction (RT-PCR). For N-terminal sequencing, the antibodies were first run on SDS/PAGE gels and then transferred to PVDF membranes (Invitrogen). The heavy and light chains were cut out of the blots and sent for sequencing (Columbia University Protein Core). For the 11f10 and 6a7 antibodies, the N-terminal sequences of the light chains were determined to be DVVMTQTPLSS and DVVMTQTP, respectively, and those of the heavy chains were DVQLQESGLGLVK and DVQLQESGP, respectively. The N-terminal sequences were input into the International Immunogenetics Information System (IMGT, http://imgt.cines.fr/) and possible germline precursors determined. Light chains were suggested to be IGKV1-131, IGKV1-132, IGKV1-133, or IGKV1-135, and heavy chains suggested to be IGHV3-2, IGHV3-5, or IGHV3-6. N-terminal DNA primers were ordered based on the N-termini of these genomic precursors, as were constant region C-terminal primers based on isotyping of the antibodies, which suggested both antibodies had κ light chains and IgG2a heavy chains. The sequences of the N-terminal primers were IgVK1-132, 5′-gatgttgtgatgacccaga-3′; IgVH3-a, 5′-gatgtgcagcttcaggag-3′; IgVH3-d, 5′-gatgtacagcttcaggag-3′. The sequences of the C-terminal primers were IGKC reverse, 5′-acactcattcctgttgaagc-3′, and IgG2A Hinge reverse, 5′-ttgattgtgggccctctg-3′. Total cellular RNA was then prepared from the respective murine hybridoma cells using RNeasy (Qiagen) and was used in one step RT-PCR reactions (Qiagen) with the above primers. Reactions which yielded DNA PCR products were sequenced to give the final sequences of the light and heavy chains, which were then read into the IMGT database and determined to be isogenic descendents of genomic precursors IGKV1-135-01 and IGHV3-2-02, respectively, and putatively of IGKJ1-01 and IGHJ3-01 J-regions and IGHD2-1-01 D-regions. Affinity matured residues of 11f10 and 6a7 were determined based on observed sequence changes to precursor V-regions.

Preparation of Antigen-Binding Fragments of Antibodies 2F5, 11f10, 6a7. Antibody Fabs of 2F5, 11f10, and 6a7 were prepared as previously described (14, 15). Briefly, antibody IgGs were first reduced with 100 mM DTT for 1 h at 37 °C, followed by 1 h of dialysis in PBS or Hepes, pH 7.6, to reduce the DTT concen-

tration to 1 mM. Antibodies were then dialyzed against 2 mM Iodoacetamide for 48 h at 4 °C, and subjected to a final dialysis against PBS or Hepes, pH 7.6, for 2 h. After reduction and alkylation, antibodies were cleaved with Lys-C (Roche), run over a Protein A column to segregate away the Fc fragment, and then subjected to ion exchange (Mono S, 2F5; Mono Q, 11f10 and 6a7) and size-exclusion chromatography.

Crystallizations.

ES2 scaffold.

We observed that the full length ES2 scaffold was prone to proteolysis at Arg271, and since the resulting N-terminal proteolytic fragment was stable, a stop codon was introduced after Arg271 and the shorter fragment was expressed and purified as described above. Crystallizations using 576 conditions adapted from the commercially available Hampton (Hampton Research), Precipitant Synergy (Emerald Biosystems), and Wizard (Emerald Biosystems) crystallization screens were set up robotically (Honeybee) using vapor diffusion sitting drops. Robotic crystal hits were hand optimized and crystals that were grown in 23% PEG 4000, 120 mM $(NH_4)_2SO_4$, 20 mM ATP at 20 °C diffracted to 2.8 Å resolution.

ES2:2F5 Fab complex.

Purified 2F5 Fab was incubated with excess ES2 (Arg271) scaffold for 0.5 h at 25 °C and the complex was then loaded onto a gel filtration column (Superdex 200). A clear peak could be discerned for the complex and crystallizations were set up robotically as described for free ES2. Crystal hits were hand optimized, and crystals grown in 16% PEG 400, 2.8% PEG 3350, 100 mM sodium acetate ($C_2H_3NaO_2$), pH 5.5, 20 mM ATP, diffracted to 2.5 Å, though were only 33% complete in the highest resolution shell.

11f10:gp41-peptide and 6a7:gp41-peptide complexes.

Threefold molar excess of gp41 peptide LLELDKWA corresponding to residues 660–667 of gp41 (HxB2 numbering) was added to purified 11f10 and 6a7 Fabs and the complexes set up for robotic crystallization, as described above. For the 11f10:gp41 complex, crystal hits were hand optimized and those grown from 16% PEG 4000, 80 mM sodium acetate ($C_2H_3NaO_2$), 40 mM Tris-Cl, pH 8.5 diffracted to better than 2 Å. For the 6a7:gp41 complex, crystals grown in 31.5% PEG 1000, 200 mM zinc acetate ($C_4H_{10}O_6Zn$), 100 mM sodium acetate ($C_2H_3NaO_2$), pH 4.5 diffracted to better than 2 Å, in a space group that was distinct from the 11f10:gp41 crystals.

Data Collection, Structure Solution, and Refinement. Crystals were transferred into stabilizing solutions containing 5–10% higher concentrations of precipitant and a cryoprotectant (40% glycerol for ES2, 15% 2R-3R butanediol for 11f10 and 6a7 crystals). For the 11f10 and 6a7 crystals, cryosolutions were supplemented with 4 mM gp41 peptide to ensure the peptide did not dissociate from the crystal after dilution with the cryo. After mounting the crystals on a loop, they were flash cooled and data was collected on SER CAT ID-22 or BM-22 beamlines (APS) and processed using HKL-2000 (16).

Structures were solved with molecular replacement using Amore (17, 18) or Phaser (19). For the free ES2 scaffold the parental ES2 structure 1KU2a was used as a search model. For the ES2:2F5 complex, both 1KU2a and the 2F5 crystal structure 1TJI were used as search models. For the 6a7:gp41 complex, 1BBJ was used as a search model, and the solved 6a7 model structure with a few rounds of refinement was subsequently used as a search model for 11f10:gp41.

Refinement of the ES2 and ES2:2F5 crystal structures was undertaken using CNS (20), with iterative model building using O (21). For the 11f10:gp41 and 6a7:gp41 crystal structures, Phenix (22) was used for refinement and Coot for model building (23). All structures were validated with MolProbity (32).

Structural Analyses. The program Grasp (24) was used to determine electrostatic potential maps of structural surfaces, which were then read into PyMOL (PyMOL Molecular Graphics System, Versions 0.99 and 1.2r3pre). Grasp was also used to determine exposed surface area of the non-antibody-bound face of the core five residues (662–666, HxB2 numbering) of the epitope. This was performed for epitope scaffolds ES1-ES5, and for the free and cyclized peptides. In each case, 2F5-bound and unbound surface areas were calculated for the whole ligand molecule. The exposed surface area of the core five residues was defined as the area contributed by the core residues to the nonbound surface.

To determine spatial overlap of antibody Fv fragments, the antibodies were superimposed using an alignment of their respective complexed gp41 peptides. The total volume enfolding both antibody Fvs was then determined using Grasp, and the percent overlap defined as the mean volume of the individual Fvs divided by the volume of their superposition.

Structural alignments were performed using the program lsqkab (ccp4 Package (25)). Difference-distance matrix calculations were determined using Differences Distance Matrix Plot (DDMP) software, as previously described (26) [Fleming, P. http://www.roselab.jhu.edu/ddmp/ (2004)]. MS, PISA, and HBPLUS were used to determine contact surfaces and residues (27–29). All structural figures were generated with use of PyMOL (Versions 0.99 and 1.2r3pre).

1. Siever E, Spainhour S, Figgins S, & Hekman JP (2000) *LINUX in a Nutshell* (O'Reilly & Associates, Inc., Sebastopol, CA) 3rd Ed p 797.
2. Berman HM et al. (2000) The Protein Data Bank. *Nucleic Acids Res* 28(1):235–242.
3. Wang G & Dunbrack RL, Jr. (2003) PISCES: A protein sequence culling server. *Bioinformatics* 19(12):1589–1591.
4. Ortiz AR, Strauss CE, & Olmea O (2002) MAMMOTH (matching molecular models obtained from theory): An automated method for model comparison. *Protein Sci* 11(11):2606-2621.
5. Kuhlman B & Baker D (2000) Native protein sequences are close to optimal for their structures. *Proc Natl Acad Sci USA* 97(19):10383–10388.
6. Kuhlman B et al. (2003) Design of a novel globular protein fold with atomic-level accuracy. *Science* 302(5649):1364–1368.
7. Campbell EA et al. (2002) Structure of the bacterial RNA polymerase promoter specificity sigma subunit. *Mol Cell* 9(3):527–539.
8. Kambach C et al. (1999) Crystal structures of two Sm protein complexes and their implications for the assembly of the spliceosomal snRNPs. *Cell* 96(3):375–387.
9. Dunbrack RL, Jr. & Cohen FE (1997) Bayesian statistical analysis of protein side-chain rotamer preferences. *Protein Sci* 6(8):1661–1681.
10. Gray JJ et al. (2003) Protein-protein docking with simultaneous optimization of rigid-body displacement and side-chain conformations. *J Mol Biol* 331(1):281–299.
11. Barouch DH et al. (2005) A human T-cell leukemia virus type 1 regulatory element enhances the immunogenicity of human immunodeficiency virus type 1 DNA vaccines in mice and nonhuman primates. *J Virol* 79(14):8828–8834.
12. Mackenzie D, Arendt A, Hargrave P, Mcdowell JH, & Molday RS (1984) Localization of binding-sites for carboxyl terminal specific antirhodopsin monoclonal-antibodies using synthetic peptides. *Biochemistry* 23(26):6544–6549.
13. Chakrabarti BK et al. (2005) Expanded breadth of virus neutralization after immunization with a multiclade envelope HIV vaccine candidate. *Vaccine* 23(26):3434-3445.
14. Chen L et al. (2009) Structural basis of immune evasion at the site of CD4 attachment on HIV-1 gp120. *Science* 326(5956):1123–1127.
15. Ofek G et al. (2004) Structure and mechanistic analysis of the antihuman immunodeficiency virus type 1 antibody 2F5 in complex with its gp41 epitope. *J Virol* 78(19):10724–10737.
16. Otwinowski Z & Minor W (1997) Processing of X-ray diffraction data collected in oscillation mode. *Method Enzymol* 276:307–326.
17. Navaza J (1994) Amore—An automated package for molecular replacement. *Acta Crystallogr A* 50:157–163.
18. Bailey S (1994) The CCP4 Suite—Programs for protein crystallography. *Acta Crystallogr D* 50:760–763.
19. Mccoy AJ et al. (2007) Phaser crystallographic software. *J Appl Crystallogr* 40:658–674.
20. Brunger AT et al. (1998) Crystallography & NMR system: A new software suite for macromolecular structure determination. *Acta Crystallogr D* 54(Pt 5):905–921.
21. Jones TA, Zou JY, Cowan SW, & Kjeldgaard M (1991) Improved methods for building protein models in electron-density maps and the location of errors in these models. *Acta Crystallogr A* 47:110–119.

22. Adams PD et al. (2002) PHENIX: Building new software for automated crystallographic structure determination. *Acta Crystallogr D* 58:1948–1954.
23. Emsley P & Cowtan K (2004) Coot: Model-building tools for molecular graphics. *Acta Crystallogr D* 60:2126–2132.
24. Nicholls A, Sharp KA, & Honig B (1991) Protein folding and association: Insights from the interfacial and thermodynamic properties of hydrocarbons. *Proteins* 11(4): 281–296.
25. Kabsch W (1976) Solution for best rotation to relate 2 sets of vectors. *Acta Crystallogr A* 32(Sep1):922–923.
26. Huang CC et al. (2005) Scorpion-toxin mimics of CD4 in complex with human immunodeficiency virus gp120: Crystal structures, molecular mimicry, and neutralization breadth. *Structure* 13(5):755–768.
27. Connolly ML (1993) The molecular-surface package. *J Mol Graphics* 11(2):139–143.
28. Krissinel E & Henrick K (2007) Inference of macromolecular assemblies from crystalline state. *J Mol Biol* 372(3):774–797.
29. McDonald IK & Thornton JM (1994) Satisfying hydrogen-bonding potential in proteins. *J Mol Biol* 238(5):777–793.
30. Wright SP (1992) Adjusted p-values for simultaneous inference. *Biometrics* 48(4): 1005–1013.
31. Benjamini Y & Hochberg Y (1995) Controlling the false discovery rate—A practical and powerful approach to multiple testing. *J Roy Stat Soc B Met* 57(1):289–300.
32. Chen VB et al. (2010) MolProbity: All-atom structure validation for macromolecular crystallography. *Acta Crytallogr D* 66:12-21.

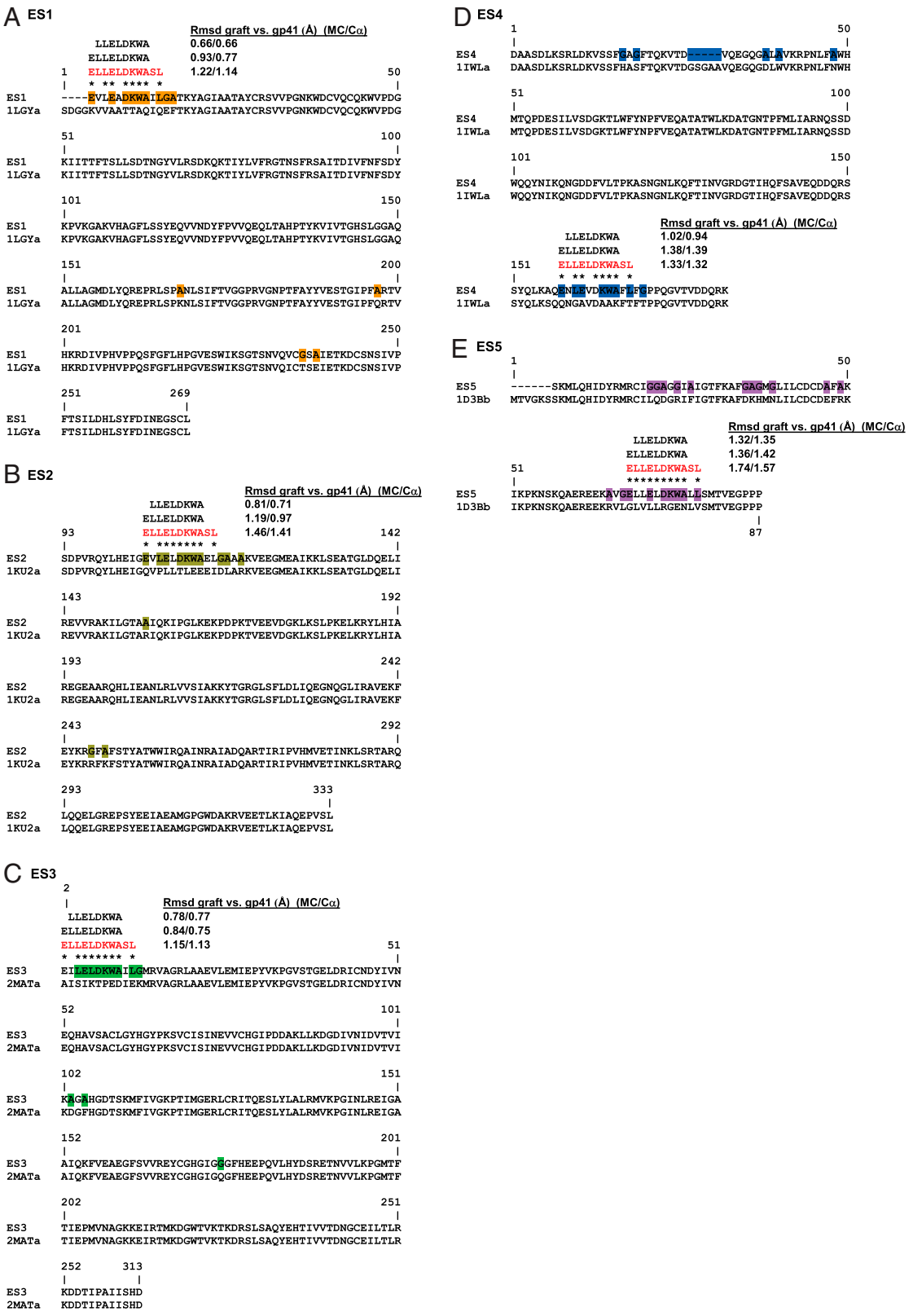

Fig. S1. Sequences of 2F5-epitope scaffolds. Shown are alignments of the amino acid sequences of epitope scaffolds ES1, (*A*), ES2, (*B*), ES3, (*C*), ES4, (*D*), and ES5, (*E*), with their parental proteins, labeled based on PDB ID code. Residues that were mutated from the parental sequence to build in the gp41 graft or accommodate 2F5-binding are shaded. The sequence of gp41 residues 659–669 (red), upon which the grafting was based, is aligned onto the graft of each scaffold, with residues of gp41 that are present in the graft labeled with asterisks. Root-mean-square deviations (rmsd) of the epitope graft against gp41 residue ranges 660–667, 659–667, and 659–669 from PDB ID 1TJI are shown for main-chain (MC) and Cα atoms.

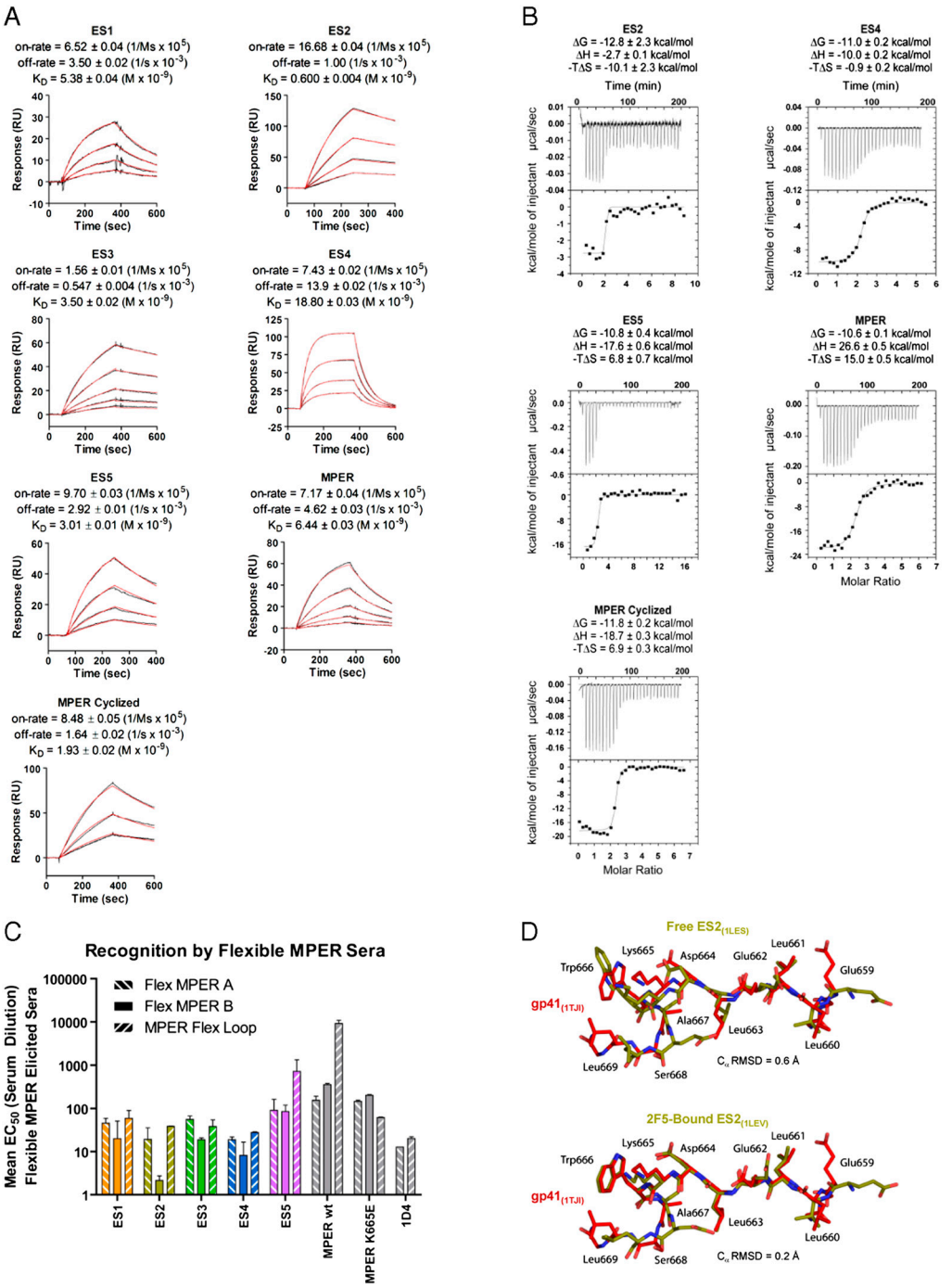

Fig. S2. Experimental characterization of epitope scaffolds. (*A*) Surface–plasmon resonance analysis of 2F5 Fab binding to epitope scaffolds. To determine binding affinities of epitope scaffolds to antibody 2F5 Fab, epitope scaffolds ES1-ES5 were directly immobilized onto Biacore CM5 sensor chips and 2F5 Fab was flowed over as analyte. For affinities to wild type and cyclized MPER-C9 peptides, 2F5 IgG was directly immobilized onto the sensor surface and the peptides flowed over as analyte. Shown sensograms, black, are twofold serial dilutions of 2F5 Fab at concentrations 0.97–7.8 nM (ES1), 0.49–3.9 nM (ES2), 0.97–15.6 nM (ES3), 1.95–15.6 nM (ES4), and 0.49–3.9 nM (ES5), or peptide analyte concentrations of 0.49–7.8 nM (MPER-C9) and 1.95–7.8 nM (MPER-C9-cyclized). Sensograms were fit with a 1:1 Langmuir model, shown in red. (*B*) Thermodynamics of interaction between 2F5 and epitope scaffolds. Shown are isothermal titration calorimetry profiles (VP-ITC, Microcal) of 2F5 IgG with epitope scaffolds ES2, ES4, and ES5, and with wild-type and cyclized MPER-C9 peptides. In all experiments shown, 2F5 IgG was placed into the calorimeter cell at a concentration of 1–2 μM, and the scaffolds or peptides injected as ligands. Effective concentrations of the ligands were 40 μM, ES2, 24 μM, ES4, 135 μM, ES5, 25 μM, MPER-C9 WT peptide, and 30 μM, MPER-C9 cyclized peptide (see *SI Materials and Methods*). After baseline adjustment, the profiles were fit using Origin Ver. 7.0 (Microcal), and the results are presented in each panel and in Table 1. (*C*) Recognition of epitope scaffolds by flexible MPER-elicited serum. ELISA mean EC_{50}s of flexible MPER-elicited serum recognition of epitope scaffolds ES1-ES5 and of wild-type and point mutant K665E MPER peptides are shown (flexible MPER A serum, left slanting hatch, flexible MPER B serum, solid bars, MPER flexible loop serum, right slanting hatch). As a negative control, reactivity with 1D4 antibody was also examined (for flexible MPER A and MPER flexible loop sera), and served as a reference baseline. All experiments were performed in duplicate. (*D*) Shown are superpositions of residues 659–669 of gp41 in its 2F5-bound conformation (red) against corresponding residues (105–115) of the epitope graft in the crystal structure of unliganded ES2 (top, yellow) and 2F5-bound ES2 (bottom, yellow). Root-mean-square deviations (rmsd, Å) of Cα atoms are listed in each case.

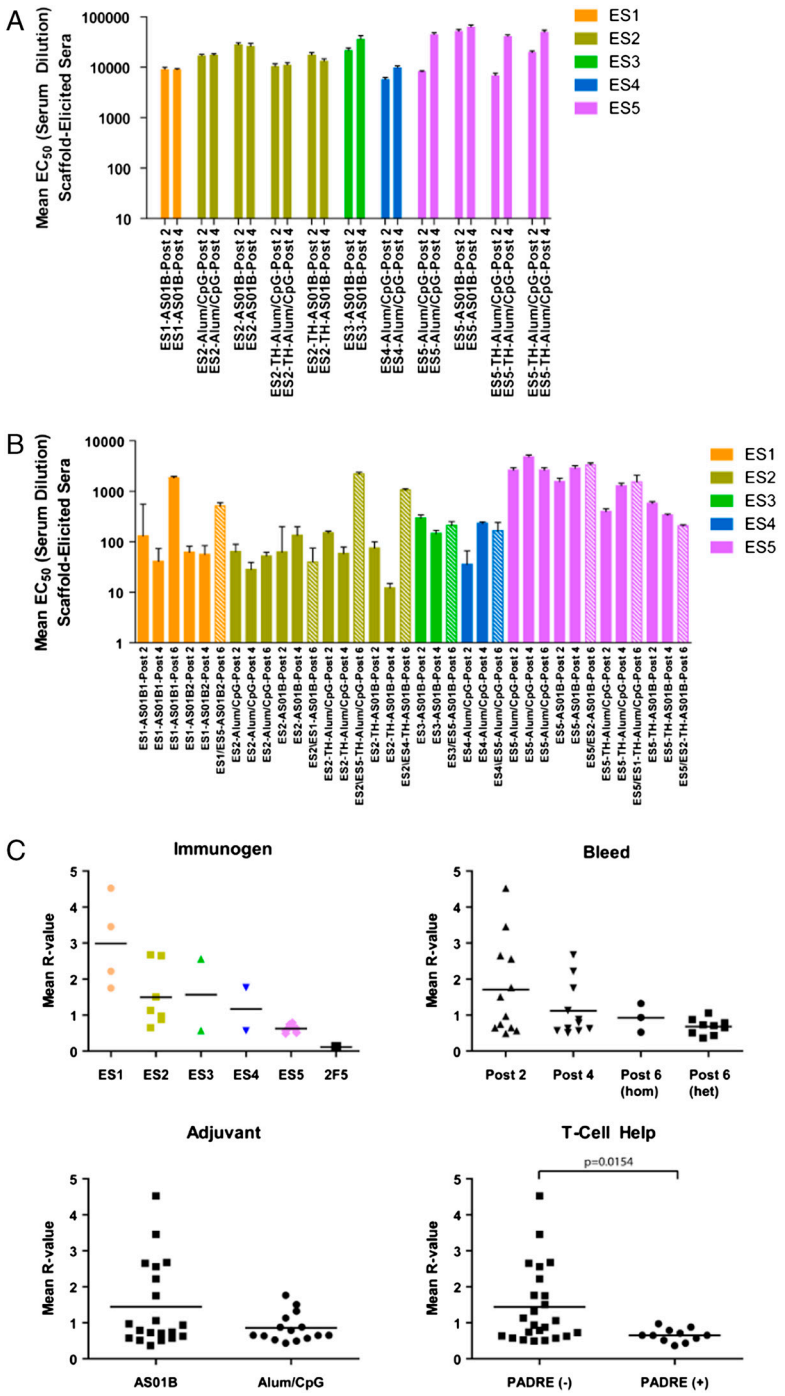

Fig. S3. Characterization of epitope-scaffold-elicited sera. (*A*) Overall responses elicited by epitope scaffolds. Sera elicited by epitope scaffolds were examined for antibody titers against the entire respective scaffolds (including regions outside of the graft). Post 2 and Post 4 bleeds of all animal groups shown in Fig. 2*A*, with the exception of group 2, were analyzed in ELISA format for reactivity with the respective scaffold immunogen. Shown are EC_{50} values obtained by fitting ELISA profiles with four parameter logistic curves (GraphPad Prism Version 5.0). (*B*) Graft-specific responses of scaffold-elcited sera. Sera elicited by epitope scaffolds were also examined for graft-specifc immune responses, using reactivity to MPER-C9 peptide. ELISAs were performed and analyzed as in *A*, for Post 2, 4, and 6 bleeds of all animal groups. For Post 6 samples, hatched bars indicate heterologous boosts for the last two immunizations, while solid bars indicate homologous boost. All ELISA experiments were performed in duplicate. (*C*) Factors influencing the quality of 2F5 epitope-scaffold-elicited responses. Alanine scan profiles of all serum samples were grouped based on different parameters used in the immunizations—immunogen, bleed, T-cell help, or adjuvant. Mean *R*-values per group were then examined for effects of each parameter, with the lower the *R*-values the closer the mimicry to the alanine scan profile of 2F5 (see *SI Materials and Methods*). Shown, clockwise from upper left, are mean *R*-values per immunogen (for post 2 and post 4 immunizations), per serum bleed (with post 6 profiles separated based on whether the boosts were homologous or heterologous), per adjuvant, and per presence of a T-cell helper epitope (PADRE). For reference, the *R*-values for sera elicited by MPER in flexible formats were 1.02 ± 0.01 and 0.87 ± 0.02, for flexible MPER immunized rabbits A and B, respectively, and 0.91 ± 0.03 and 1.19 ± 0.04 for cyclized MPER immunized rabbits 1 and 2, respectively.

A

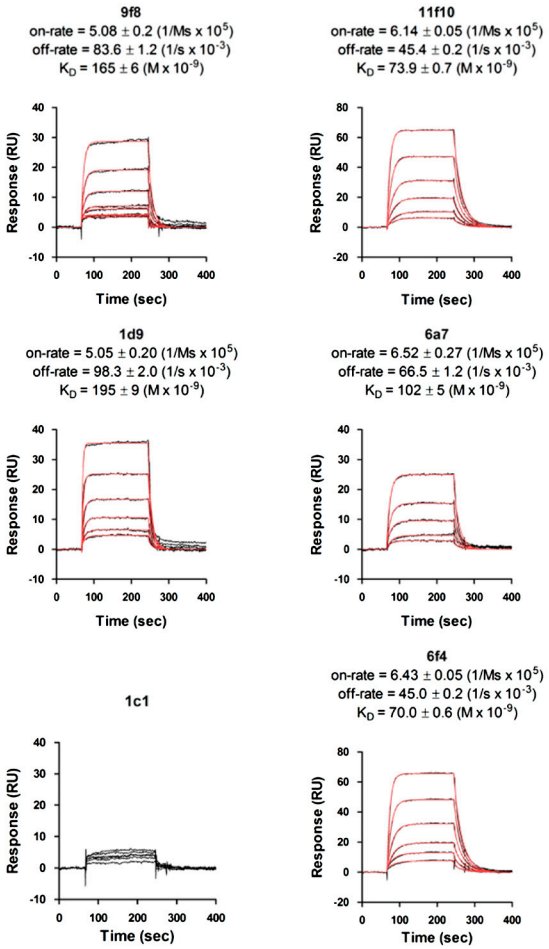

C

Comparison of Angles of Approach to gp41.

Fv	Volume* (Å^3)	%-Overlap†
$2F5_{1TJI}$	42200	na
$2F5_{2P8M}$	40500	na
$6a7_{3LEY}$	41800	na
$11f10_{3LEXa}$	41500	na
$11f10_{3LEXb}$	41400	na
$2F5_{1TJI}$ + $2F5_{2P8M}$	44500	92.9
$2F5_{1TJI}$ + $6a7_{3LEY}$	52400	80.2
$2F5_{1TJI}$ + $11f10_{3LEXa}$	52100	81.3
$2F5_{1TJI}$ + $11f10_{3LEXb}$	52100	80.2

*Volumes determined using the program Grasp (24).

†%-Overlap defined as the ratio between the mean volume of the individual Fv's with the volume of their superposition.

na, not applicable.

B

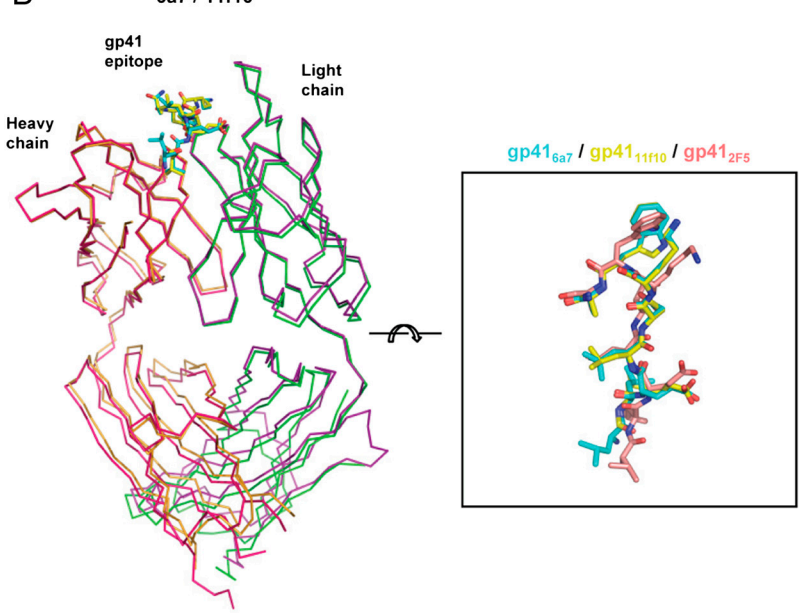

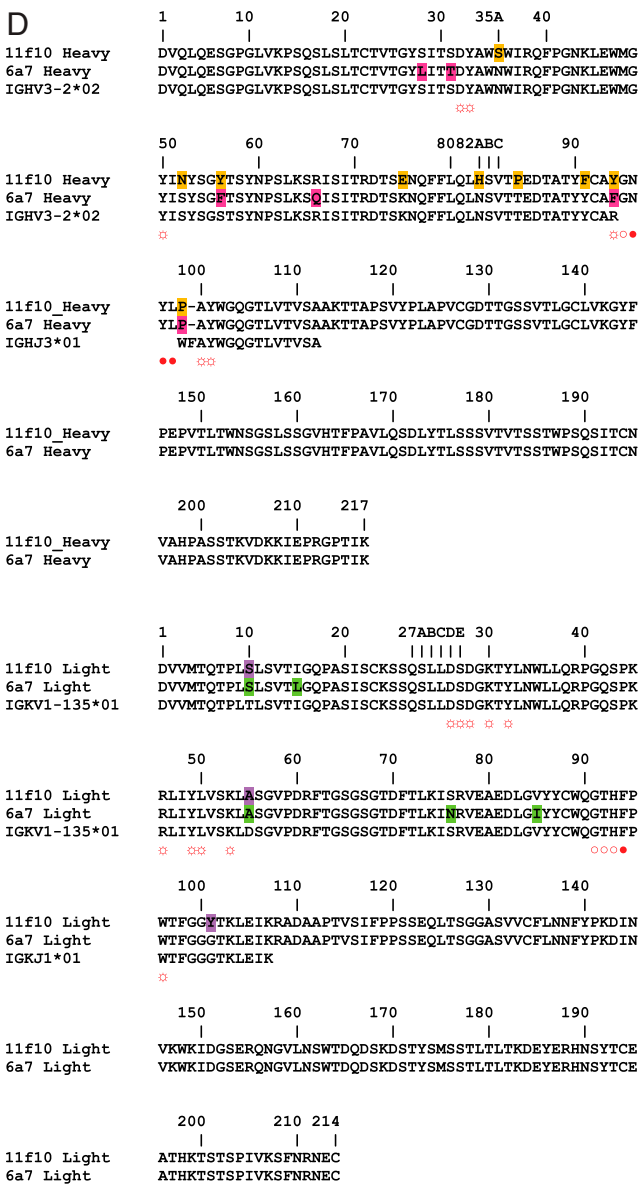

Fig. S4. Characterization of epitope-scaffold-elicited monoclonal antibodies. (*A*) Surface–plasmon resonance analysis of binding of elicited monoclonal antibodies to gp41 peptide. Monoclonal antibodies elicited by homologous immunization with the ES5 epitope scaffold—9f8, 1d9, and 1c11—and those elicited by heterologous immunization with epitope scaffolds ES5 and ES1—11f10, 6a7, and 6f4—were directly immobilized onto Biacore CM5 sensor chips and the gp41 MPER-C9 peptide was flowed over as analyte. Twofold increasing concentrations of analyte were used, ranging from 3.9–125 nM (11f10, 6f4), 3.9–62.5 nM (6a7), 0.97–125 nM (9f8), and 15.6–500 nM (1d9, 1c11). Sensograms, black, were fit with a 1:1 Langmuir model, red. Binding constants are reported in each panel, with the exception of 1c1 antibody, for which biding to peptide was too low to obtain proper values at the concentrations tested. (*B*) Structure of monoclonal antibody 6a7 in complex with gp41. Shown in the left panel is a backbone representation of the crystal structure of the 6a7 Fab (heavy chain, magenta; light chain, green) in complex with the gp41 peptide LLELDKWA (cyan). The crystal structure of the isogenically related antibody 11f10 (heavy chain, orange; light chain, purple) in complex with gp41 peptide (yellow) is superimposed. A closeup view of the alignment of all atoms of the gp41 peptides from the 6a7 and 11f10 crystal structures against corresponding residues of 2F5-bound gp41 (salmon) is shown on the right. (*C*) Comparison of angles of approach to gp41. To compare angles of approach to gp41 of the elicited and 2F5 antibodies, spatial overlap of the antibody Fv fragments relative to gp41 was determined. The antibody Fvs were first oriented by superimposing their complexed gp41 peptides, and then the total volume enfolding them both was determined. Percent-overlap was calculated by dividing the mean volume of the two individual Fv's by the volume of their superposition. (*D*) Sequences, progenitor genes, and affinity maturation of antibodies 11f10 and 6a7. Shown are sequence alignments of the heavy and lights chains of monoclonal antibodies 11f10 and 6a7, against their common heavy and light chain precursors. Residues that are shaded (orange, 11f10 heavy chain; magenta, 6a7 heavy chain; purple, 11f10 light chain; green, 6a7 light chain) are different from their genomic precursor at that position. Antibody residues that contact gp41 peptide in the crystal structures are labeled with red circles (open circles, main-chain contacts only; open circles with rays, side-chain contacts only; closed circles, both main-chain and side-chain contacts).

Table S1. Crystallographic data and refinement statistics

	ES2	ES2:2F5-Fab	11f10:gp41$_{660-667}$	6a7:gp41$_{660-667}$
Crystallographic Data				
Space group	*P*1	$P2_12_12_1$	*P*1	$P2_1$
Unit cell dimensions				
a (Å)	37.3	58.5	34.5	36.2
b (Å)	50.0	63.9	70.9	80.2
c (Å)	57.6	200.0	78.3	72.1
α (°)	78.0	90	90.1	90
β (°)	89.8	90	90.0	97.1
γ (°)	87.6	90	90.3	90
Resolution (Å)*	48.9 – 2.77(2.87 – 2.77)	46.1 – 2.50(2.59 – 2.50)	50.00 – 1.97(2.04 – 1.97)	50.00 – 1.98(2.05 – 1.98)
Number of reflections	18235	210613	98782	83950
Unique reflections*	9968 (940)	23675 (862)	49925 (5030)	26922 (2394)
Completeness (%)*	95.9 (89.4)	88.9 (33.1)	94.6 (94.7)	96.7 (86.9)
I/σ*	15.0 (1.5)	42.9 (1.17)	33.0 (12.9)	31.5 (5.2)
R_{sym}(%)†	6.2 (41.1)	9.0 (47.0)	3.8 (9.2)	8.1 (34.2)
Refinement statistics ($F > 0$)				
Non-hydrogen atoms				
total	2880	5000	7459	3736
peptide	2832	4819	6783	3405
water	28	97	676	331
ligand	20	84		
Resolution (Å)	48.86-2.77	46.15-2.50	25.90-1.97	27.10-1.99
$R_{crystal}$ (%)‡	22.65	20.05	16.47	17.67
R_{free} (%)‡	26.03	25.28	19.75	21.55
Rmsd bond length (Å)	0.004	0.007	0.009	0.004
Rmsd bond angles (°)	0.751	0.959	0.892	0.768
Average B-factor (Å^2)	87.1	85.2	26.9	41.8
PDB ID	3LES	3LEV	3LEX	3LEY

*Data in parentheses are for highest resolution shell.
†$R_{sym} = \sum |(I_{obs} - I_{avg})| / \sum I_{avg}$
‡$R = \sum_{hkl} |(|F_{obs}| - |F_{calc}|)| / \sum_{hkl} |F_{obs}|$

Table S2. Structural comparison of free and 2F5-bound ES2 grafts to 2F5-bound gp41

Rmsd (Å) of gp41 Residues 660–667/659–667/659–669*

	gp41$_{1TJI}$			gp41$_{2P8M}$			ES2$_{Parental1KU2a}$			ES2$_{Model}$			ES2$_{3LESa}$			ES2$_{3LESb}$			ES2:2F5$_{3LEV}$		
gp41$_{1TJI}$				0.3	0.5	na	0.7	1.0	1.4	0.7	1.0	1.4	0.6	1.0	1.3	0.6	1.0	1.3	0.2	0.7	1.3
gp41$_{2P8M}$	0.4	0.8	na				0.7	1.1	na	0.7	1.0	na	0.6	1.1	na	0.6	1.1	na	0.4	0.9	na
ES2$_{Parental1KU2a}$	0.8	1.2	1.5	0.8	1.2	na				0.1	0.1	0.1	0.5	0.5	0.6	0.5	0.5	0.6	0.7	0.7	0.7
ES2$_{Model}$	0.8	1.2	1.5	0.8	1.2	na	0.1	0.1	0.1				0.5	0.5	0.5	0.5	0.5	0.5	0.6	0.6	0.6
ES2$_{3LESa}$	0.7	1.2	1.3	0.7	1.2	na	0.5	0.5	0.5	0.5	0.5	0.5				0	0	0	0.6	0.6	0.6
ES2$_{3LESb}$	0.7	1.2	1.3	0.7	1.2	na	0.5	0.5	0.5	0.5	0.5	0.5	0	0	0				0.6	0.6	0.6
ES2:2F5$_{3LEV}$	0.5	1.0	1.4	0.6	1.1	na	0.6	0.6	0.6	0.7	0.7	0.6	0.5	0.5	0.5	0.5	0.5	0.5			

Difference-distance matrix means of gp41 Residues 660–667/659–667‡,§

	gp41$_{1TJI}$		gp41$_{2P8M}$		ES2$_{Parental1KU2a}$		ES2$_{Model}$		ES2$_{3LESa}$		ES2$_{3LESb}$		ES2:2F5$_{3LEV}$	
gp41$_{1TJI}$			0.2	0.5	0.4	0.5	0.4	0.6	0.4	0.6	0.2	0.4	0.4	0.4
gp41$_{2P8M}$	0.1	0.3			0.5	0.8	0.4	0.9	0.4	0.9	0.3	0.8	0.5	0.8
ES2$_{Parental1KU2a}$	0.3	0.3	0.3	0.5			0.5	0.5	0.5	0.5	0.3	0.4	0.0	0.0
ES2$_{Model}$	0.3	0.4	0.3	0.6	0.3	0.3			0.0	0.0	0.4	0.4	0.4	0.4
ES2$_{3LESa}$	0.3	0.4	0.3	0.6	0.3	0.3	0.0	0.0			0.4	0.4	0.4	0.5
ES2$_{3LESb}$	0.1	0.2	0.2	0.5	0.2	0.2	0.3	0.3	0.3	0.3			0.3	0.3
ES2:2F5$_{3LEV}$	0.3	0.3	0.3	0.5	0.0	0.0	0.3	0.3	0.3	0.3	0.2	0.2		

*In each subsection, rmsd of main-chain atom (N, Cα, C) superpositions shown in lower left, and rmsd of Cα atom superpositions shown in upper right. Row and column headings correspond to PDB IDs used in the respective superpositions. Alignments of gp41 residues 660–667 are shaded red, 659–667 blue, and 659–669 yellow.
†Rmsds calculated using the program lsqkab (25).
‡Mean difference of absolute values shown in lower left; Root-mean-square difference shown in upper right. Row and column headings correspond to PDB IDs used in the respective calculations. Results for gp41 residues 660–667 and 659–667 are shaded red and blue, respectively.
§Difference-distance matrix means were determined using Differences Distance Matrix Plot (DDMP) software, as previously described [(26), Fleming, P. http://www.roselab.jhu.edu/ddmp/].

Table S3. Interactive surface areas on 2F5 and gp41 in the ES2, 11f10, and 6a7 crystal structures

2F5 (residue)	2F5 Interactive Surface Area* with gp41/ES2$_{3LEV}$ (Å^2)			2F5 (residue) cont'd	2F5 Interactive Surface Area* with gp41/ES2$_{3LEV}$ (Å^2)		
	gp41$_{2P8M}$	gp41$_{1TJI}$	ES2$_{3LEV}$		gp41$_{2P8M}$	gp41$_{1TJI}$	ES2$_{3LEV}$
Ala$_{L1}$	11	11	12	Asp$_{H54}$	13	17	21
Leu$_{L2}$	18	25	22	Asp$_{H56}$	15	15	28
Gln$_{L3}$	0	4	0	Arg$_{H58}$	19	20	33
Ser$_{L26}$	0	5	0	Tyr$_{H59}$	0	0	4
Gln$_{L27}$	20	44	16	Pro$_{H61}$	0	0	7
Gly$_{L28}$	0	1	0	Arg$_{H95}$	28	28	32
Thr$_{L30}$	0	1	0	Arg$_{H96}$	5	7	5
Leu$_{L91}$	10	11	11	Gly$_{H97}$	3	3	3
His$_{L92}$	40	41	39	Pro$_{H98}$	22	33	21
Phe$_{L93}$	53	50	53	Val$_{H100d}$	0	0	31
Tyr$_{L94}$	74	74	84	Pro$_{H100e}$	0	16	35
Pro$_{L95}$	4	2	10	Ile$_{H100f}$	0	13	0
His$_{L96}$	8	9	10	Ala$_{H100g}$	0	20	0
Phe$_{H32}$	10	11	9	Arg$_{H100h}$	0	70	43
Gly$_{H33}$	21	29	25	Gly$_{H100i}$	0	1	0
Tyr$_{H52}$	31	39	40	Val$_{H100k}$	22	26	26
Ser$_{H53}$	0	0	4	Asn$_{H100l}$	3	4	2
Subtotal	300	357	335		130	273	291
Total	430	630	626				

gp41/graft Residue	gp41/Graft Interactive Contact Surface Area (Å^2)					
	11f10$_{3LEXa}$†	11f10$_{3LEXb}$†	6a7$_{3LEY}$†	2F5$_{1TJI}$†	2F5$_{3LEV}$	2F5$_{2P8M}$†
Glu$_{657/103}$				13		
Gln$_{658/104}$				20		
Glu$_{659/105}$				17	8	15
Leu$_{660/106}$	1	1	14	0	0	0
Leu$_{661/107}$	80	81	86	67	75	69
Glu$_{662/108}$	51	48	45	57	57	60
Leu$_{663/109}$	23	23	26	35	37	45
Asp$_{664/110}$	52	54	54	65	59	66
Lys$_{665/111}$	56	58	58	63	71	67
Trp$_{666/112}$	93	94	88	98	105	85
Ala$_{667/113}$	29	29	32	29	28	12
Ser$_{668/114}$				0	10	0
Leu$_{669/115}$				51	29	0
Trp$_{670/116}$				37	17	0
Asn$_{671/117}$				7	0	0
Total	385	387	402	560	496	419
Total (gp41$_{660-667}$)	385	387	402	415	431	404
Acidic (gp41$_{660-667}$)	103	101	98	123	116	126
Basic (gp41$_{660-667}$)	56	58	58	63	71	67
Hydrophobic (gp41$_{660-667}$)	226	228	246	229	245	212

*Molecular contact surface areas by residue represent sums of main-chain and side-chain contact surfaces, as determined by the program MS (27).

†The residue ranges of the gp41 peptides are: 1TJI (654-670-[N-Ac]), 2P8M (659-671), 3LEX (660-667-[N-Ac]), 3LEY (660-667-[N-Ac]).

Table S4. Hydrogen bonds and salt bridges between gp41 and antibodies 11f10, 6a7, and 2F5

		Distance* (Å)				Distance* (Å)		
gp41/ES2$_{3LEV}$ (Atom)†	11f10/6a7 (Atom)	gp41:11f10 (3LEXa)	gp41:11f10 (3LEXb)	gp41:6a7 (3LEY)	2F5 (Atom)	gp41:2F5 (1TJI)	gp41:2F5 (2P8M)	ES2:2F5 (3LEV)
$Gln_{658}O$					$Gln_{L27}N\varepsilon2$	3.2		
$Glu_{659}O\varepsilon2$					$Ala_{L1}N$	2.9	3.2	
$Leu_{661}N$	$Tyr_{H33}OH$	3.4	3.4	3.3				
$Leu_{661}O$	$Asn_{H96}N\delta2$	3.1	3.0	3.3				
$Glu_{662}O/Glu_{108}O$					$Tyr_{L94}N$	2.8	3.0	2.9
$Glu_{662}O\varepsilon2$	$Tyr_{L50}OH$			3.4	$Arg_{H58}NH2$	2.8	2.5	
$Glu_{662}O\varepsilon1$	$Tyr_{L50}OH$	3.2	2.9		$Arg_{H58}N\varepsilon$	2.8	2.6	
$Asp_{664}O\delta1/Asp_{110}O\delta1$	$Tyr_{H97}N$			2.8	$His_{L96}N\varepsilon2$	2.8	2.6	2.9
$Asp_{664}O\delta1/Asp_{110}O\delta1$	$Leu_{H98}N$	2.8	2.8		$Arg_{H95}NH1$	2.8	3.2	3.0
$Asp_{664}O\delta2/Asp_{110}O\delta2$	$Leu_{H98}N$			3.0	$Arg_{H95}NH2$	2.9		2.9
$Asp_{664}O\delta2/Asp_{110}O\delta2$	$Tyr_{H97}N$	2.9	2.9					
$Asp_{664}N/Asp_{110}N$	$Asn_{H96}O$	3.0	2.9	2.9	$His_{L92}O$	2.9	2.6	2.7
$Lys_{665}N/Lys_{111}N$					$Tyr_{L94}OH$	3.3	3.2	3.3
$Lys_{665}N\zeta$	$Thr_{L92}O$	2.8	2.8	3.0	$Asp_{H54}O\delta1$	2.8		
$Lys_{665}N\zeta$	$Asp_{L27d}O\delta1$	2.7	2.7	2.6	$Asp_{H56}O\delta1$	2.9		
$Trp_{666}O$					$Arg_{H100h}N$			
$Trp_{666}N\varepsilon1$	$Gly_{L91}O$	2.6	2.6	2.6				
$Ala_{667}O$					$Arg_{H100h}N$			
$Trp_{670}O$					$Arg_{H100h}N$	2.9		
Total Contacts $gp41_{660-667}$		9	9	9		10	7	6

*Hydrogen bonds and salt bridges and corresponding distances determined using HBPLUS (29).
†The residue ranges of the gp41 peptides are: 1TJI (654-670-[N-Ac]), 2P8M (659-671), 3LEX/3LEY (660-667-[N-Ac]).

Table S5. Individual and grouped *R*-factors for alanine-interrogated epitope-scaffold-elicited responses

Individual sera*	Mean *R*-value	SE†	*p*-value (Bootstrap)	*p*-value (Bonferroni‡)	*p*-value (FDR‡, §)	Grouped sera	Mean *R*-value	*p*-value (Bootstrap)	*p*-value (Bonferroni‡)	*p*-value (FDR‡, §)
2F5.MAb	0.12	0.01	0.00000	0.00000	0.00000	ES1	2.23	0.99896	1.00000	0.99994
ES2.TH.AS01B.Post.6	0.36	0.04	0.00005	0.00278	0.00070	ES2	1.21	0.94379	1.00000	0.99994
ES2.TH.Alum.CpG.Post.6	0.44	0.03	0.00057	0.03294	0.00659	ES3	1.40	0.97995	1.00000	0.99994
ES5.Alum.CpG.Post.2	0.49	0.04	0.00265	0.15358	0.02560	ES4	1.07	0.86575	1.00000	0.99994
ES1.AS01B2.Post.6	0.51	0.02	0.00401	0.23246	0.03080	ES5	0.64	0.05532	1.00000	0.20758
ES5.TH.AS01B.Post.4	0.51	0.03	0.00425	0.24638	0.03080	Flexible Peptide¶	1.00	0.78277	1.00000	0.99994
ES5.Alum.CpG.Post.6	0.53	0.02	0.00582	0.33733	0.03748	Post 2	1.71	0.99511	1.00000	0.99994
ES4.Alum.CpG.Post.4	0.57	0.01	0.01591	0.92290	0.08279	Post 4	1.12	0.90425	1.00000	0.99994
ES5.TH.AS01B.Post.2	0.57	0.12	0.01600	0.92800	0.08279	Post 6 (homologous)	0.93	0.66051	1.00000	0.99994
ES3.AS01B.Post.4	0.57	0.00	0.01713	0.99342	0.08279	Post 6 (heterologous)	0.68	0.09990	1.00000	0.28970
ES5.AS01B.Post.4	0.63	0.03	0.04415	1.00000	0.19699	T-Help (+PADRE)	0.65	0.06715	1.00000	0.20758
ES5.Alum.CpG.Post.4	0.63	0.08	0.04938	1.00000	0.20459	T-Help (−PADRE)	1.38	0.97805	1.00000	0.99994
ES5.TH.Alum.CpG.Post.2	0.65	0.17	0.06030	1.00000	0.20758	AS01B	1.45	0.98441	1.00000	0.99994
ES2.TH.Alum.CpG.Post.2	0.65	0.02	0.06553	1.00000	0.20758	Alum/CpG	0.86	0.49461	1.00000	0.99994
ES5.TH.Alum.CpG.Post.6	0.65	0.01	0.06800	1.00000	0.20758					
ES5.TH.AS01B.Post.6	0.71	0.11	0.14207	1.00000	0.39239					
ES2.AS01B.Post.6	0.73	0.16	0.17907	1.00000	0.47210					
ES5.AS01B.Post.2	0.74	0.01	0.20521	1.00000	0.51748					
ES5.TH.Alum.CpG.Post.4	0.79	0.01	0.30667	1.00000	0.71458					
ES5.AS01B.Post.6	0.79	0.01	0.30801	1.00000	0.71458					
Flexible MPER B	0.87	0.02	0.51290	1.00000	0.99994					
ES4.Alum.CpG.Post.6	0.88	0.05	0.54114	1.00000	0.99994					
ES2.TH.Alum.CpG.Post.4	0.88	0.07	0.54802	1.00000	0.99994					
Flexible MPER Cyc1	0.91	0.03	0.62683	1.00000	0.99994					
ES1.AS01B1.Post.6	0.93	0.04	0.67272	1.00000	0.99994					
ES2.TH.AS01B.Post.2	0.97	NA	0.74286	1.00000	0.99994					
Flexible MPER A	1.02	0.01	0.81178	1.00000	0.99994					
ES3.AS01B.Post.6	1.06	0.37	0.85527	1.00000	0.99994					
ES2.Alum.CpG.Post.4	1.13	0.14	0.90893	1.00000	0.99994					
Flexible MPER Cyc2	1.19	0.04	0.93626	1.00000	0.99994					
ES2.Alum.CpG.Post.6	1.32	0.18	0.97022	1.00000	0.99994					
ES2.Alum.CpG.Post.2	1.51	0.10	0.98843	1.00000	0.99994					
ES1.AS01B2.Post.4	1.75	0.59	0.99575	1.00000	0.99994					
ES4.Alum.CpG.Post.2	1.76	NA	0.99594	1.00000	0.99994					
ES1.AS01B1.Post.4	2.22	0.24	0.99891	1.00000	0.99994					
ES3.AS01B.Post.2	2.56	NA	0.99949	1.00000	0.99994					
ES2.AS01B.Post.2	2.65	NA	0.99958	1.00000	0.99994					
ES2.AS01B.Post.4	2.68	NA	0.99959	1.00000	0.99994					
ES1.AS01B2.Post.2	3.46	NA	0.99988	1.00000	0.99994					
ES1.AS01B1.Post.2	4.52	1.39	0.99994	1.00000	0.99994					
ES2.TH.AS01B.Post.4	NA	NA	NA	NA	NA					

*For Post 6 samples, scaffold for immunizations 5 and 6 is listed if heterologous (see Fig. 2*A*).

†SE, standard error.

‡Bootstrap *p*-values were adjusted due to multiple comparisons, as described in (30).

§*p*-values computed using a step-up False Discovery Rate procedure, as described in (31). Significant results have a false discovery rate of 3.75%.

¶Flexible peptide group includes Flexible MPER A, B, Cyc1, and Cyc2 sera.

NA, not applicable.

Red, statistically significant *p*-values.